Estuarine, Coastal and Shelf Science (2000) **50,** 39–48
Article No. ecss.1999.0530, available online at http://www.idealibrary.com on IDEAL®

Maximizing Information from a Water Quality Monitoring Network through Visualization Techniques

J. N. Boyer[a,c], P. Sterling[a] and R. D. Jones[a,b]

[a]*Southeast Environmental Research Center, Florida International University, Miami, FL 33199, U.S.A.*
[b]*Department of Biological Sciences, Florida International University, Miami, FL 33199, U.S.A.*

Received 19 January 1999 and accepted in revised form 26 February 1999

This paper describes a variety of visualization techniques that have been very useful for demonstrating important aspects of a water quality monitoring programme in South Florida. The first level of visualization was at the single station or grouped stations using the box-and-whisker plot as a graphical/statistical tool. This plot was used to compare intra-annual variability and correlation between total phosphorus (TP) and chlorophyll *a* (chl *a*) at a site in Florida Bay. Secondly, time was added as a dimension to produce a 9-year, monthly time series plot of declining salinity at a site in NE Florida Bay. It was shown how a centred moving average could be used to smooth out the noise and disclose inter-annual oscillations. Time series of anomalies from long term means were discussed as a means of displaying correspondence and coupling among variables. Thirdly, the utility of 2-D contour maps of variables was demonstrated in showing sources and mixing of fresh water across the hydroscape as well as nutrient loading to the South Florida ecosystem. From this expanded spatial view, it was observed that the water quality of different bays and coastal areas are differentially affected both by external and internal processes and how management of pump operations and canal conductance can overwhelm the natural hydrological cycle and have far reaching impacts in Florida Bay and the SW Florida Shelf. We also showed that contouring was useful for elucidating causal relationships among variables over the spatial domain. Time step animations of monthly salinity contours in Florida Bay showed the importance of mixing with western boundary waters to alleviation of hypersaline conditions. These animations also showed that it is the shifting lags between TP concentration and chl *a* which make it so difficult to derive a simple regression model. Finally, a 3-D volumetric rendering of the area between Key West and the Tortugas was used to describe a strong density stratification event during July 1998 and to visualize the source of water masses and general circulation patterns in this region. It is concluded that visualization techniques are useful not only to show patterns in the data but in developing new hypotheses for future research and monitoring activities.

Keywords: water quality; estuary, geostatistics; salinity; nutrients; chlorophyll; Florida Bay; coral reef; management

Introduction

The purpose of most water quality monitoring programmes is to assess the status and trends in ambient water quality of the study area. Many of these programmes are operated by government organizations or consulting firms and focus on regulatory requirements. Often the publications begin with a map of the sampling stations and then go on to describe the temporal variability of each water quality variable station by station. In reading this type of report, the reader rapidly becomes mired in a confusing wilderness of data tables, bar charts and line graphs. What is most often lost in the process are the spatial relationships of the data; the relationships among stations close together as compared to those far apart.

Humans are inherently visually-oriented animals; a large percentage of our brains is delegated to processing visual signals. One of the most powerful aspects of visualization software is the ability to zoom out from the narrow field of view of the individual station to a more holistic view of the hydroscape or ecosystem. This approach is aided by the capacity to combine datasets from contiguous areas of study to produce one ' big picture ' of the region. In this paper we present a hierarchical approach to visualizing both temporal and spatial aspects of ambient water quality using our monitoring programme in South Florida as an example. This is in no way the only way to go about mining information from data but it is an approach that has

Full sized figures, tables and animations are stored on the CD-ROM accompanying this article. Use a Web browser to access the start page ' default.htm ' and follow the links. The help file ' help.htm ' provides answers for some common problems.
[c]E-mail: boyerj@fiu.edu

worked well for us in disseminating information to outside users.

Methods

Data collection and analysis

The data come from six separate water quality monitoring programmes in South Florida as funded by the South Florida Water Management District (SFWMD), Everglades National Park (ENP) and Environmental Protection Agency (EPA). The estuarine portion of the network consists of 28 fixed sampling stations in Florida Bay, 22 stations in Whitewater Bay, 25 stations in Biscayne Bay, and 25 stations in the Ten Thousand Islands (Figure 1). The coastal section includes water quality data collected from 154 stations within the Florida Keys National Marine Sanctuary (FKNMS) and 49 stations located on the SW Florida Shelf (Shelf).

Each of the estuarine stations were sampled on a monthly basis beginning in March 1991 at stations 1 through 24 in Florida Bay (monitoring began at stations 14, 19, 22 and 23 in April 1991). Additional data during 1990–91 were collected by Bugden (1993) and incorporated into the database. In July 1992, stations 25 through to 28 were added in Florida Bay to better cover the western boundary. Whitewater Bay was added to the monitoring programme in September 1992, Biscayne Bay in September 1993, and Ten Thousand Islands sampling began September 1994. The FKNMS and Shelf were sampled on a quarterly schedule beginning in March 1995.

Field sampling of the estuaries included surface (10 cm) and bottom salinity (using the Practical Salinity Scale), temperature (°C), and dissolved oxygen (DO, $mg\,l^{-1}$). Salinity and temperature were measured using a combination salinity-conductivity-temperature probe (Orion model 140). DO was measured using an oxygen electrode (Orion model 840) corrected for salinity and temperature. Periodic measurements of *in situ* photosynthetically available radiation (PAR, $\mu E\,m^{-2}$), were made using a Li-Cor irradiance meter equipped with two 4π spherical sensors (LI-193SB) separated by 0·5 m in depth and oriented at 90° to each other. The sensors were calibrated in air and then used to measure instantaneous difference between sensors in the water column which was then used to calculate the vertical light attenuation coefficient (K_d, m^{-1}). Field measurements on the shelf included salinity, temperature, and DO in surface water only. Field variables in the FKNMS were measured using CTD casts (Seabird SBE 19) at each station and resulted in depth profiles of salinity, temperature, DO, PAR, chlorophyll *a* specific fluorescence (volts), optical backscatterance turbidity, depth measured by pressure transducer (m), and density (σ_t, $kg\,m^{-3}$).

Water samples from the estuaries and shelf were collected, in duplicate, from the surface only (*c.* 10 cm). In the FKNMS, water was collected from *c.* 0·25 m below the surface and at *c.* 1 m from the bottom with a Teflon-lined Niskin bottle (General Oceanics) except in the shallow backcountry area of the Lower Keys where only surface samples were collected. Filtered water samples (Whatman GF/F) were analysed for the dissolved nutrients nitrate (NO_3^-), nitrite (NO_2^-), ammonium (NH_4^+), and soluble reactive phosphate (SRP). The filters themselves were extracted with 90% acetone/10% water and analysed for chlorophyll *a* (chl *a*, $\mu g\,l^{-1}$) by spectrofluorometry. Specific fluorescence from the CTD was converted to chl *a* using a regression equation between voltage and extracted chl *a* developed from >700 field samples. Unfiltered water samples were analysed for total concentrations of organic nitrogen (TON), organic carbon (TOC), phosphorus (TP), silicate ($Si(OH)_4$), turbidity (NTU), and alkaline phosphatase activity (APA; $\mu M\,h^{-1}$). Detailed analytical procedures are provided in Boyer *et al.* (1997). All nutrient concentrations were reported in uM unless noted otherwise.

Visualization techniques

Several different examples of data visualization are presented with the overall approach being a progression through increasing hierarchical scales:

(a) 1-D single station or group—box-and-whisker plot
(b) 1-D_t single station or group over time—time series line graph
(c) 2-D spatial analysis of region—contour maps (snapshot in time)
(d) 2-D_t spatial analysis of region over time—time series animation of contour maps
(e) 3-D volumetric region - transparent droplet with isosurface slicing animation.

Box-and-whisker plots were generated using StatView (Abacus Concepts) although other software packages have this capability. The box-and-whisker plot is a powerful statistic which displays the median, range and the shape of the data distribution. Water quality variable distributions are usually skewed to the right (non-normal) so it is more appropriate to use the median as the measure of central tendency. The central, horizontal line of the box is the median of the data, the top and bottom of the box are the 25th and 75th percentiles (quartiles), the ends of the whiskers are the 10th and 90th percentiles, and any points outside (<10th and >90th percentiles) may be considered outliers. The box-and-whisker plot may also serve as a graphical, nonparametric ANOVA. The notch in the box is the 95% confidence interval of the median. When notches among boxes do not overlap, the medians may be considered significantly different. As this is a visual test, differences between sites are usually confirmed using the nonparametric paired Wilcoxon Ranked Sign test (comparable to the paired *t*-test) and among sites by the Kruskall–Wallace test (ANOVA).

Time series plots were produced using Excel (Microsoft). Often raw time series data look noisy and are difficult to interpret. One method of smoothing the data is to calculate a centred moving average ($X_t = X_{n+1}/2 + X_{n+2} + \ldots + X_{n+(z-1)} + X_{n+z}/2$) where z=window width, and overlay it on the graph. The moving average acts as a low pass filter to disclose long-term oscillations and allows visual assessment of the linearity of trends (Chatfield, 1989). A 12-month moving average was chosen because we were interested in inter-annual signals but any period may be specified.

Contour maps were produced using Surfer (Golden Software). The most important aspect of generating contour maps is the geostatistical algorithm used for interpolating the data values. Several different algorithms are usually supplied with the software, e.g. inverse distance, polynomial regression, kriging, etc. Care should be taken in the selection of the algorithm because automated interpolation to a regular rectangular grid can produce artifacts, especially around the edges and when the area of interest is irregularly shaped. The safest approach is to verify the point pattern of the contour with a dummy dataset prior to analysis. Kriging is often the algorithm of choice because it is designed to minimize the error variance while at the same time maintaining point pattern continuity (Isaaks & Srivastava, 1989). Kriging is a global approach which uses standard geostatistics to determine the ‘ distance ’ of influence around each point and the ‘ clustering ’ of similar samples sites (autocorrelation). Therefore, unlike the inverse distance procedure, kriging will not produce valleys in the contour between neighbouring points of similar value.

The time series animations were produced using Surfer by writing a macro which accessed the archived data file, read the data from the first sampling survey, grided the data to a regular array, produced a contour mask for a selected variable, overlaid it on a map template, and exported it as a GIF file. This procedure was iterated through the database until there were *c.* 120 separate files. The individual GIF files were then combined into a FLC file by a freeware program, Dave’s Targa Animator and compiled into an animation. The animation was originally run from our website (http://www.fiu.edu/~serc/jrpp/wqmn/datamaps/datamaps.html) using a stand-alone freeware program, Autodesk Animation Player for Windows 1.0 (Autodesk Inc.). For standardization purposes, the FLC movie was converted to a 320 × 240 AVI file using Motion Video Cross-Compiler 1.6 (by Bob Williamson). The result of all these manipulations was the production of short AVI clips of monthly data from Florida Bay, kriged as contour plots, running from 1989 to 1998 at two frames per second.

The 3-D animation was produced using Tecplot 7.5 (Amtec Engineering). The 34 CTD casts were used to define the depth boundaries for the volume. This greatly simplified the animation process because we did not need to integrate a bathymetric map with the data. Ideally, and in the future, bathymetry will be included but because of the good coverage of CTD casts it was not a requirement.

Results and discussion

1-D single station or group—box-and-whisker plot

The first level of visualization was that of the individual station or statistically grouped stations (Boyer *et al.*, 1997). This is simply a visualization of descriptive statistical characteristics of the data from one or more sites. The method of choice for this comparison is the box-and-whisker plot which allows a great deal of flexibility because we can compare not only the distribution of a single continuous variable but also compare the distribution of groups as defined by nominal values. Figure 2 shows TP and chl *a* data from one station in Whitewater Bay grouped by a nominal variable, month of year, for the entire 6-year period of record. This visualization method is excellent at showing intra-annual variability in the data, e.g. some months have very high concentrations and wide ranges in TP and chl *a* (February) while others have much lower concentrations and less variability (August). In certain cases, the variability around the median may be quite large resulting in the 95% confidence interval notch being wider than the interquartile range. Note that both TP and chl *a* track each other over the annual cycle and are significantly related (P<0·0001), but this regression is not very useful as a predictive model ($R^2=0{\cdot}38$).

1-D$_t$ single station or group over time—time series line graph

Another method of visualizing information from a station or group of stations is to present the data as a time series (Figure 3). The example provided shows the salinity at a site in NE Florida Bay, being composed of 9-years of monthly sampling events. It is clear that there has been a declining trend in salinity at this site; which has been confirmed for the whole eastern region of Florida Bay as well (Boyer *et al.*, 1999). In addition to the overall decline, a periodicity to the trend was observed which correlated with precipitation patters and water management activities (Boyer & Jones, 1999).

Another important type of information available from a long-term programme is the temporal anomalies of the variables. Anomalies are departures from the long-term mean and are easily calculated by subtracting the mean from the monthly data. Sea surface temperature anomalies have been shown to be critical in predicting the onset of El Niño/Southern Oscillation events (Philander, 1990). The plot of the precipitation anomaly showed the cycling signal of the wet and dry seasons as well as the interannual differences between wet and dry years (Figure 4). To understand how this might affect estuarine salinity it must be known how precipitation affects terrestrial runoff in this region.

The northern boundary of Florida Bay is composed of the Everglades marsh with the eastern Everglades integrated into the Taylor Slough watershed and C-111 coastal basin (Figure 1). In addition to precipitation, there is a managed canal system which pumps water into Taylor Slough through the S-18C structure on a defined schedule (Light & Dineen, 1994). The output from Taylor Slough and the C-111 coastal basin is a significant source of fresh water to NE Florida Bay and has been shown to be driven by climate and management (Smith *et al.*, 1989; Walker, 1997; Boyer & Jones, 1999). The overlay of the freshwater flow anomaly showed a strong increase over time (Figure 4). This uncoupling of flow from local rainfall is due in part to management activity of pump operation (Boyer & Jones, 1990). Therefore, S-18C flow was a more reliable proxy for freshwater input from the Everglades than was precipitation alone because it incorporated management activity into the equation. It is also important to note that the management activity of pump operations and canal conductance can overwhelm the natural hydrological cycle and that man's modification of the watershed has far reaching impacts to the receiving waters of Florida Bay.

2-D spatial analysis of bay—contour maps

Many research and monitoring programmes have relied on the use of contouring to show the spatial relationships among sites during synoptic sampling events. A contour map supplies an overall view of important spatial properties but may miss significant features due to coarseness of the grid and mask small variations by having the contour levels set too high. The first problem arises from lack of spatial resolution due to under-representation of sampling sites. This problem can only be rectified by increased effort and funding. The second problem of masking may become evident when studying a highly heterogeneous system with large sources and sinks but can be corrected by plotting contour intervals using a log scale. Therefore, it is important that contour maps be viewed only as ' helpful qualitative displays with questionable quantitative significance ' (Isaaks & Srivastava, 1989).

The contour example (Figure 5) shows ' snapshots ' of both salinity and NO_3^- concentrations in Biscayne Bay for May 1997. It can be seen that the release of fresh water from the canal system on the SW shore resulted in a significant depression in salinity over an extensive area of the bay. Notice also that NO_3^- is elevated in this region as a direct result of increased freshwater loading. The impacts of this freshwater pulse are mitigated in central Biscayne Bay by tidal exchange with the Atlantic Ocean across the mouth (called interestingly enough, the Safety Valve). This kind of visual information showing the effects of canal management on conditions in the bay makes a much greater impact on policymakers and the public than could any table of numbers.

We have also experimented with expanding the areal coverage by incorporating data from adjacent monitoring programmes to produce regional, semi-synoptic maps of water quality (Figure 6). For this figure data have been combined from six separate monitoring programmes, all sampled during the same month. Care must be taken to standardize methodology and to minimize the amount of time it takes to complete the field sampling. The assumption that large scale patterns in water quality variables are robust over the sample collection time has been tested using overlapping sites collected at different times within the month. This approach is subject to variability occurring over time scales shorter than the sample collection time (mostly tidal, advective and biological), but we have found it to be much less than the variability between sampling events.

The contour map of salinity across the South Florida hydroscape (Figure 6) shows active freshwater sources, seawater mixing zones and potential advective transport through the region. The main freshwater sources of Shark and Taylor Sloughs as well as the transport of lower salinity water of the shelf south along western Florida Bay and out through the passes in the Keys can be seen. From this expanded view, we observe that the water quality of different bays and coastal areas are directly affected both by external nutrient transport and internal nutrient source/sinks (J. Boyer, unpubl. data). This large-scale visualization illustrates an important point; that individual political/management boundaries should not be thought of as enclosing distinct ecosystems. It also points out how water management activities may overwhelm natural hydrologic conditions.

Contouring is also useful for elucidating causal relationships among variables. For example, the spatial distribution of P limitation potential can be illustrated by plotting the regression coefficient (R^2) of the relationship between TP concentration and chl *a* for all sampling events to date (Figure 7). Those areas with high R^2 values, central Florida Bay, the Shelf and the Marquesas (west of Key West), are identified as regions where P inputs may be most important in driving phytoplankton primary production. Visualization then becomes a tool not only to show patterns in the data but to aid in the development of new hypotheses for planning future research and monitoring activities.

2-D_t spatial analysis of bay or region over time—time series animation of contour maps

The next obvious step in the visualization process is to produce time series animations of contoured data. Since we had the longest record for Florida Bay, it was decided to assemble the monthly sampling events into a simple movie clip. Salinity was chosen (Animation 1), chl *a* (Animation 2), and TP (Animation 3) as interesting examples for this visualization approach. Our original time series analysis showed that salinity in Florida Bay had declined from the hypersaline peaks of 1989–91 to more normal estuarine salinities to date (Boyer *et al*., 1999). An interesting aspect of Animation 1 is that it clearly shows that salinity first began to decline in the NW and NE bay and eventually spread to the central region (see from July–November 1991). Therefore, the alleviation of hypersalinity in Florida Bay resulted not only from terrestrial freshwater inputs in the east (Taylor Slough) but from mixing with the shelf at the western boundary. Smith *et al*. (1989) showed that the Shark Slough, which exits through the west coast mangrove estuaries, may be more important to salinity in the bay overall than the Taylor Slough. We previously showed (Figure 6) that fresh water from the Shark Slough decreased the nearshore salinity on the shelf and that this water may be transported south to western Florida Bay and out through the Keys (Smith, 1994; Lee *et al*., 1998). Therefore, the salinity of Florida Bay is tied to the output of the Shark Slough via fluctuating salinity of the shelf and its effects on mixing at the western boundary.

Along with hypersalinity, Florida Bay experienced large blooms of phytoplankton in the north central and western zones during 1992–95 (Animation 2). The algal blooms began almost one year after a major seagrass die-off (Robblee *et al*., 1991) provoking speculation that they were fuelled by remineralization of dead seagrass biomass. It is important to recognize that the bottom topography of Florida Bay is more like an assemblage of discrete basins interconnected by shallow, narrow passes than the typical coastal plain estuary with a longitudinal channel. This physical isolation between basins allows the development of discrete blooms of differing community structure to occur at different times in different basins (Phlips & Badylak, 1996). Some bloom events were short lived with chl *a* concentrations being high one month and very low the next; other bloom events persisted much longer and covered a larger area. The most striking aspect of the 1992–95 blooms were that many of them occurred in the winter months, during the dry season.

Lastly, the time series of TP concentrations (Animation 3) showed striking similarities to that of chl *a*. Running both TP and chl *a* animations in concurrent mode allows us to compare these similarities in space and time. The lags between TP concentration buildup and phytoplankton biomass become evident. Sometimes TP is high before the bloom starts then declines as it develops; other times a bloom develops with no prior increase in TP or it persists for long periods after TP has declined. The discrepancy arises as a function of sampling frequency; it is unrealistic to expect a monthly sampling regime to unravel the complex interaction between TP and phytoplankton which operates on shorter time scales (TP—hourly/daily and phytoplankton—weekly/monthly).

Another important aspect of the spatial distribution of TP was that most of the high concentrations appeared at those stations closest to the coast in the central and NW bay (Animation 3). This is of interest because this area of the bay receives very little freshwater runoff due to the Buttonwood Ridge which runs parallel to the coast on the southern edge of the Everglades. Periodic water runoff through this area occurs during high water events (Swain, 1998) but no significant groundwater source to north-west Florida Bay has been identified (D. Corbett, unpubl. data; R. Price, unpubl. data.).

3-D volumetric region—slicing animation with isosurface

The last visualization approach shown is a 3-D volume representation of the area of the FKNMS extending from Key West to the Dry Tortugas National Park (Animation 4). This animation shows the salinity in this region over 12–13 July 1998. We chose this specific sampling period for the demonstration because it occurred during an interesting stratification event.

The animation begins by displaying the surface contour map and depth face on the Florida Straits side of the FKNMS at an oblique angle, like the top and edge of a desk. This view clearly shows a surface layer of lower salinity (*c.* 34) in and around the Tortugas which increased with depth in the Florida Straits to *c.* 36. This view also shows that surface salinity increased in the direction of Key West over the shallow Quicksands and Marquesas islands. As the slicing animation progresses along the axis of longitude, it becomes clear that the strongest salinity stratification occurred on the north side of the Tortugas Channel, between the shallow Tortugas and Rebecca Shoals at the edge of the Quicksands. This stratification event was strongly driven by temperature differences as well; bottom temperatures were significantly lower than surface in this area (Table 1).

As the animation proceeds along the horizontal plane, the denser bottom waters are seen to spill out through the Tortugas Channel into the Florida Straits. We believe the colder, high salinity water was most likely moving SW through the Tortugas Channel and mixing with water in the Florida Straits. The net transport of bottom water had to be from north to south because the Atlantic Ocean water was of intermediate salinity and more vertically mixed than that on the Shelf. Since the high density bottom water was being transported SW through the Tortugas Channel, it was postulated that the surface water might be moving in an opposite direction as counterflow. Viewing Animation 4 as it slices along the latitudinal axis we observe strong stratification west of the Tortugas which separates around the islands and reforms over the Tortugas Channel. By slowly stepping through the horizontal plane with the pause button, one notices a tongue of lower salinity water that extend NE from the Florida Straits onto the Tortugas. We postulate that

TABLE 1. Median values of water quality variables measured at the surface and bottom of the water column at stations selected as $\Delta\sigma_t$>0·5 kg m^{-3} during a density stratification event 12–13 July 1998. Statistical differences between surface and bottom values (P<0·100) was ascertained using the nonparametric paired Wilcoxon Ranked Sign test (bold). Salinity is reported in practical salinity units all other variables are in μM unless noted otherwise

	Surface	Bottom	P
Salinity	**34·25**	**35·95**	<0·0001
Temperature (°C)	**30·7**	**23·6**	<0·0001
NO_3^-	**0·008**	**0·068**	0·0920
NO_2^-	**0·025**	**0·049**	0·0015
NH_4^+	0·474	0·524	NS
TON	**8·098**	**6·481**	0·0001
TP	0·223	0·225	NS
SRP	0·015	0·018	NS
APA (μM h^{-1})	**0·043**	**0·028**	0·0012
TOC	**199·82**	**162·74**	<0·0001
$Si(OH)_4$	**0·033**	**0·904**	0·0013
Chl *a* (μg l^{-1})	**0·245**	**1·587**	0·0008
Turbidity (NTU)	**0·160**	**0·305**	0·0040
DO_{sat} (%)	88·4	87·4	NS

the source of the low salinity water mass was from entrainment of the Gulf of Mexico Loop Current into the Tortugas Gyre, which has been shown to occur with some regularity (Lee *et al.*, 1994). The colder bottom water probably originated in the northern Gulf of Mexico which sank due to its higher density and was transported along the western coast of Florida and out through the Tortugas Channel. The buoyant high temperature/low salinity water originated from the Loop Current and was then redirected in a NE direction by the Tortugas Gyre. We believe that this stratification event was not only the result of atypically low salinity water moving NE over existing bottom waters but from a SW counterflow of cold, high salinity water along the bottom as well. This scenario is consistent with satellite observations in the northern Gulf where a central gyre was upwelling cold bottom water from the DeSoto Canyon.

The last animation (Animation 5) shows the distribution of chl *a* during the same sampling cruise. The bottom waters along the eastern boundary of the Tortugas Channel and north of the Quicksands were elevated (0·75–1·5 μg l^{-1}) as compared to the surface (<0·5 μg l^{-1}) with lowest concentrations found in the surface north of the Tortugas. Some of the increase in bottom chl *a* concentrations were undoubtedly due to the presence of significantly higher concentrations of NO_3^-, NO_2^-, and $Si(OH)_4$ (Table 1). It is difficult to determine the duration of this stratification event except to say that we observed what was probably the beginning of the event during our April sampling. Both TP or SRP were exhausted in surface and bottom waters probably as a result of biological uptake during this period. Interestingly, concentrations of organic C and N were higher in the surface layer which may be considered as further evidence of Loop Current influence.

Conclusions

We have shown the utility of various visualization approaches in educing the ' science ' out of what is often perceived as banal water quality monitoring programmes. Data visualization has helped us to better understand the sources, transport, and fate of nutrient loading to the South Florida ecosystem. Visualization techniques have also afforded us a unique perspective on the functioning and circulation patterns of the system. It has given us the ability to question the relationships among measured variables and allowed us to generate new hypotheses and avenues of research. Most of all, data visualization has been extremely useful in the dissemination of information garnered from our monitoring efforts to scientists, agencies, non-governmental organizations, politicians and the public through newsletters and the Internet.

Acknowledgements

We thank all of our many field and laboratory technicians for their diligence and perseverance in this ongoing programme. We want to thank the captains and crew of the RV *Bellows* and RV *Suncoaster* of the Florida Institute of Oceanography for their professional support of the monitoring programme and appreciate the laboratory and lodging support supplied by the Florida Program of the National Underwater Research Center, UNC-Wilmington and Keys Marine Laboratory. This work was supported by the South Florida Water Management District through Everglades National Park (SFWMD/NPS Coop. Agreement C-7919 and NPS/SERC Coop. Agreement 5280-2-9017) and by the US-EPA under Agreement #X994621-94-0. This is contribution 116 of the Southeast Environmental Research Center at Florida International University.

References

Boyer, J. N., Fourqurean, J. W. & Jones, R. D. 1997 Spatial characterisation of water quality in Florida Bay and Whitewater Bay by multivariate analysis: Zones of similar influence (ZSI). *Estuaries* **20,** 743–758.

Boyer, J. N., Fourqurean, J. W. & Jones, R. D. 1999 Seasonal and long-term trends in water quality of Florida Bay (1989–97). *Estuaries* **22,** 417–430.

Boyer, J. N. & Jones, R. D. 1999 Effects of freshwater inputs and loading of phosphorus and nitrogen on the water quality of Eastern Florida Bay. In *Phosphorus Biogeochemistry in Sub-tropical Ecosystems: Florida as a Case Example* (Reddy, K. R., O'Connor, G. A. & Schelske, C. L., eds). CRC/Lewis Publishers, Boca Raton, Florida, pp. 321–329.

Bugden, J. B. C. 1993 *Spatial and Temporal Variation of Microbial Properties in the Water Column of Florida Bay*. M.S. Thesis, Department of Biological Sciences, Florida International University, Miami, Florida.

Chatfield, C. 1989 *The Analysis of Time Series*, 5th ed. Chapman & Hall, 283 pp.

Isaaks, E. H. & Srivastava, R. M. 1989 *An Introduction to Applied Geostatistics*. Oxford Unviersity Press, Oxford, 561 pp.

Lee, T. N., Clarke, M. E., Williams, E., Szmant, A. F. & Berger, T. 1994 Evolution of the Tortugas Gyre and its influence on recruitment in the Florida Keys. *Bulletin of Marine Science* **54,** 621–646.

Lee, T. N., Johns, E., Wilson, D. & Williams, E. 1998 Florida Bay circulation and exchange study. *Proceedings of the 1998 Florida Bay Science Conference*. University of Florida Sea Grant Program.

Light, S. S. & Dineen, J. W. 1994 Water control in the Everglades: a historical perspective. In *Everglades: The Ecosystem and its Restoration* (Davis, S. M. & Ogden, J. C., eds). St. Lucie Press, pp. 47–83.

Philander, S. G. H. 1990 *El Niño, La Niña, and the Southern Oscillation*. Academic Press, New York.

Phlips, E. J. & Badylak, S. 1996 Spatial variability in phytoplankton standing stock and composition in a shallow inner-shelf lagoon, Florida Bay, Florida. *Bulletin of Marine Science* **58,** 203–216.

Robblee, M. B., Barber, T. B., Carlson, P. R., Jr., Durako, M. J., Fourqurean, J. W., Muehlstein, L. M., Porter, D., Yabro, L. A., Zieman, R. T. & Zieman, J. C. 1991 Mass mortality of the tropical seagrass *Thalassia testudinum* in Florida Bay (USA). *Marine Ecology Progress Series* **71,** 297–299.

Smith, N. P. 1994 Long-term gulf-to-Atlantic transport through tidal channels in the Florida Keys. *Bulletin of Marine Science* **54,** 602–609.

Smith, T. J., III, Hudson, J. H., Robblee, M. B., Powell, G. V. N. & Isdale, P. J. 1989 Freshwater flow from the Everglades to Florida Bay: a historic reconstruction based on fluorescent banding in the coral *Solenastrea bournoni*. *Bulletin of Marine Science* **44,** 274–282.

Swain, E. 1998 Numerical model of controlling processes at the Florida Bay coast. *Proceedings of the 1998 Florida Bay Science Conference*. University of Florida Sea Grant Program.

Walker, W. W., Jr. 1997 Analysis of water quality and hydrologic data from the C-111 basin. *Report to Everglades National Park*.

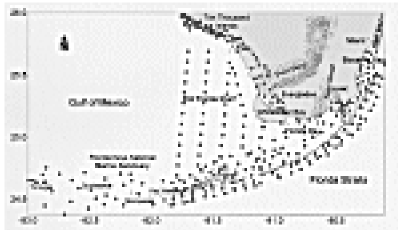

FIGURE 1. Map of South Florida ecosystem showing the 403 fixed station locations (◆) distributed throughout the various estuaries and coastal zones. This map also shows the subset of SFWMD water management canals (C-111) and pumping structures (S-18C) as well as the watershed boundaries (Taylor and Shark Sloughs) which impact Florida Bay and the SW Florida Shelf.

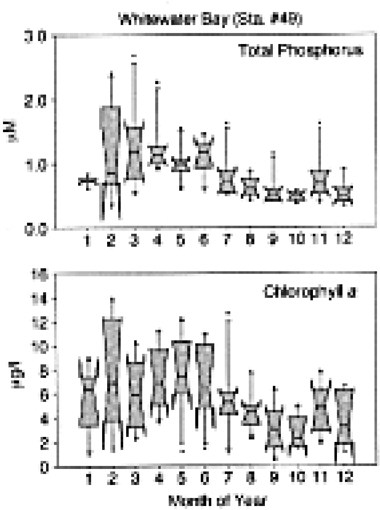

FIGURE 2. Box-and-whisker plots of total phosphorus (μM) and chlorophyll *a* ($\mu g\, l^{-1}$) concentrations for a station located in Whitewater Bay split out by month of year. The center horizontal line of the box is the median of the data, the top and bottom of the box are the 25th and 75th percentiles (quartiles), the ends of the whiskers are the 10th and 90th percentiles, and any points outside are considered outliers. The notch in the box is the 95% confidence interval of the median. When notches between boxes do not overlap, the medians may be considered significantly different. Occasionally, the 95% confidence interval of the median is wider than the range in the data much like when the standard deviation is greater than the mean.

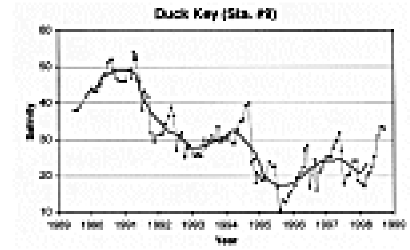

FIGURE 3. Plot of time series data of salinity decline at one site in north-eastern Florida Bay sampled monthly over a 10 year period of record. A centred, 12-month moving average (blue line) shows the presence of inter-annual oscillations and allows visual assessment of the linearity of long-term trend.

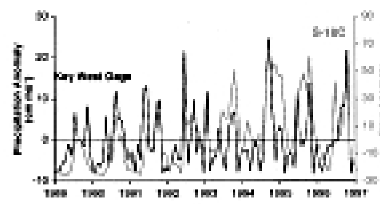

FIGURE 4. Overlay plot of precipitation anomaly (cm-month^{-1}) at Key West and freshwater flow anomaly (10^6 m^3 month^{-1}) through the S-18C pumping structure. The uncoupling of freshwater flow from local rainfall is due in part to pump operation by SFWMD.

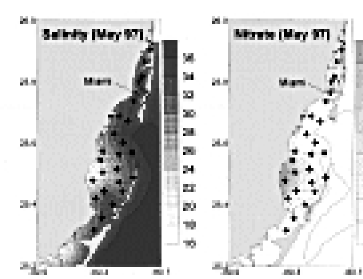

FIGURE 5. Kriged 2-D contour maps of salinity and nitrate (μM) concentrations in Biscayne Bay during the May 1997 sampling event. Clearly the freshwater output from the canal is also a source of nitrate loading to the bay.

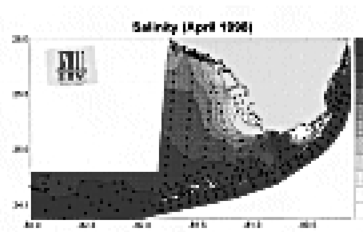

FIGURE 6. Combined contour map of salinity in the estuaries and coastal waters of the South Florida ecosystem during the April 1998 sampling event. Sources of freshwater and mixing zones are clearly portrayed by this approach.

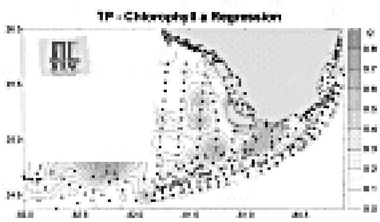

FIGURE 7. Contour map of the regression coefficient (R^2) of the relationship between TP (μM) and chl *a* (μg l^{-1}) concentrations. Those areas with high R^2 values, central Florida Bay, the shelf, and the Marquesas suggest the presence of strong P limitation of phytoplankton production.

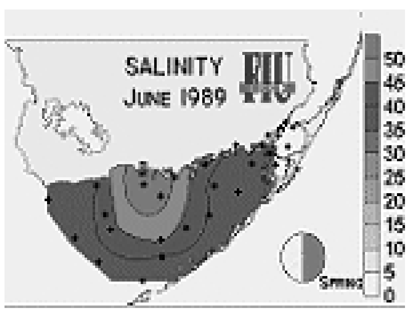

ANIMATION 1. The 2-D time series of salinity in Florida Bay shows the decline from hypersaline periods of 1989–91 to more normal estuarine salinities to date. The animation clearly shows that salinity first began to decline in the north-west and north-east bay and eventually spread to the central region (see from July–November 1991). Therefore, the alleviation of hypersalinity in Florida Bay was not only from terrestrial freshwater inputs at the head (Taylor Slough) but from mixing with the waters of the shelf at the western boundary.

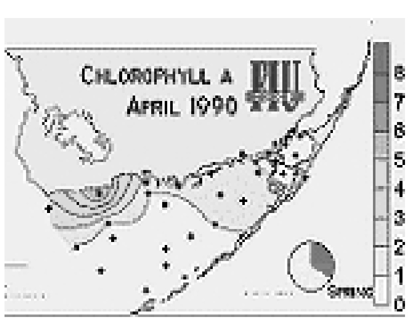

ANIMATION 2. The 2-D time series of chl *a* (μg l^{-1}) concentrations in Florida Bay shows the development and extent of phytoplankton blooms occurring in the north central and western zones during 1992–95. Notice that some bloom events were short lived with chl *a* concentrations being high one month and very low the next while other events persisted much longer and covered a much larger area.

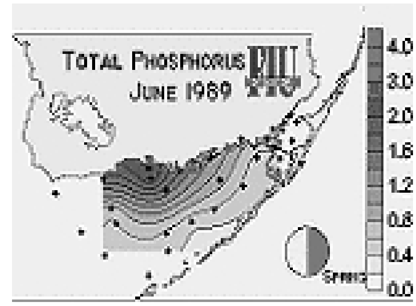

ANIMATION 3. The 2-D time series of TP (μM) shows that highest concentrations appeared at those stations closest to the north coast in the central and western Florida Bay. This is of interest because this area of the bay receives very little freshwater runoff due to the Buttonwood Ridge which runs parallel to the coast on the southern edge of the Everglades. Note the correspondence between TP and chl *a* distribution in Animation 2.

ANIMATION 4. The distribution of salinity during 12–13 July 1998 in the area of the FKNMS extending from Key West to the Dry Tortugas National Park is depicted as a 3-D volume. The 34 CTD casts are shown as vertical bars and were used to define the bottom. The animation proceeds as slices along the three axes of latitude, longitude and depth. Strongest salinity stratification occurred on the north side of the Tortugas Channel, between the shallow Tortugas and Rebecca Shoals at the edge of the Quicksands. Slices along the latitudinal axis show strong stratification west of the Tortugas which separates around the islands and reforms over the Tortugas Channel. Horizontal slices show a tongue of lower salinity water that extend NE from the Florida Straits onto the Tortugas.

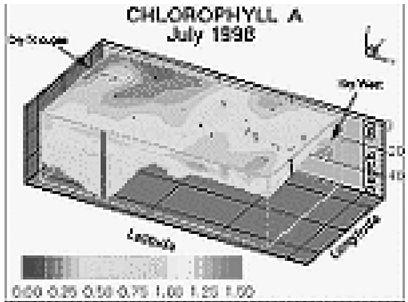

ANIMATION 5. This 3-D volumetric representation shows the distribution of chl *a* specific fluorescence ($\mu g\, l^{-1}$) in the same area of the FKNMS during the same sampling cruise. The bottom waters along the eastern boundary of the Tortugas Channel and north of the Quicksands were elevated ($0{\cdot}75$–$1{\cdot}5\ \mu g\, l^{-1}$) as compared to the surface ($<0{\cdot}5\ \mu g\, l^{-1}$) with lowest concentrations found in the surface north of the Tortugas.